
ResSVD: Residual Compensated SVD for Large Language Model Compression

Haolei Bai

Westlake University

Nanyang Technological University

Siyong Jian

Westlake University

Nanjing University

Tuo Liang

Case Western Reserve University

Yu Yin

Case Western Reserve University

Huan Wang*

Westlake University

Abstract

Large language models (LLMs) have demonstrated impressive capabilities in a wide range of downstream natural language processing tasks. Nevertheless, their considerable sizes and memory demands hinder practical deployment, underscoring the importance of developing efficient compression strategies. Singular value decomposition (SVD) decomposes a matrix into orthogonal components, enabling efficient low-rank approximation. This is particularly suitable for LLM compression, where weight matrices often exhibit significant redundancy. However, current SVD-based methods neglect the residual matrix from truncation, resulting in significant truncation loss. Additionally, compressing all layers of the model results in severe performance degradation. To overcome these limitations, we propose **ResSVD**, a new post-training SVD-based LLM compression method. Specifically, we leverage the residual matrix generated during the truncation process to reduce truncation loss. Moreover, under a fixed overall compression ratio, we selectively compress the last few layers of the model, which mitigates error propagation and significantly improves the performance of compressed models. Comprehensive evaluations of ResSVD on diverse LLM families and multiple benchmark datasets indicate that ResSVD consistently achieves superior performance over existing counterpart methods, demonstrating its practical effectiveness.

1 Introduction

Large language models (LLMs) have emerged as powerful tools, delivering state-of-the-art performance across a wide range of tasks such as text generation, translation, and reasoning. The scaling law [17] has driven a trend toward increasingly large models, exemplified by models such as GPT [4], PaLM [6], LLaMA [36], Qwen [2], and Deepseek [24], which often contain tens to hundreds of billions of parameters. Despite their powerful capabilities, the enormous scale of LLMs poses serious challenges for efficient deployment due to high computational demands [33, 38, 46]. This resource burden not only limits deployment on edge devices and consumer-level hardware but also increases the cost and carbon footprint of serving LLMs in production [29, 34].

As the scale of LLMs continues to grow, compression techniques, including weight quantization [10, 15, 22, 23], network pruning [9, 11, 25, 35], knowledge distillation [12, 40, 41, 45], and low-rank decomposition [14, 18, 21, 39, 42], have become increasingly important for the practical deployment of LLMs in resource-constrained environments. The syntactic and semantic correlations acquired during training often induce redundancy in LLM weight matrices, giving rise to a low-

*Corresponding author: wanghuan@westlake.edu.cn

rank structure [31]. As a result, singular value decomposition (SVD) provides a principled and effective approach for compressing these matrices with minimal loss. In particular, post-training approaches are gaining traction, as they can significantly reduce memory and compute requirements without the need for expensive retraining, making them especially suitable for scaling up foundation models. Recent studies on post-training SVD-based LLM compression, including ASVD [42], SVD-LLM [39], and AdaSVD [21], have made significant progress in reducing model size while preserving performance, demonstrating the effectiveness of low-rank approximation techniques in compressing LLMs. More precisely, while both ASVD and SVD-LLM apply weight matrix scaling before SVD truncation, SVD-LLM outperforms ASVD by leveraging a data whitening technique that enables a direct mapping between singular values and truncation loss. As a further advancement, AdaSVD compensates for truncation loss by iteratively updating singular matrices. However, existing methods suffer from two major limitations. First, existing methods ignore the importance of the residual matrix generated during SVD truncation, leading to significant truncation loss, as indicated by our theoretical analysis in Section 3.1. Second, compressing all model layers often results in high layer-wise error and severe error propagation, as confirmed by our results in Figure 4.

In this work, we propose **ResSVD**, a new post-training SVD-based compression method for LLMs. Building upon the two key observations outlined above, ResSVD introduces two core technical innovations. ① **Residual compensation for SVD truncation**: The residual matrix produced during SVD truncation can be effectively utilized to reduce the truncation loss. Specifically, we perform SVD truncation in two stages: we first truncate the original weight matrix \mathbf{W} to obtain its low-rank approximation \mathbf{W}_{r_1} . After that, we compute the residual matrix \mathbf{R} between \mathbf{W} and \mathbf{W}_{r_1} . Second, we apply SVD truncation to \mathbf{R} , yielding \mathbf{R}_{r_2} . Finally, we construct the compressed weight matrix $\hat{\mathbf{W}}_r = \mathbf{W}_{r_1} + \mathbf{R}_{r_2}$, where the total rank satisfies $r_1 + r_2 = r$. Theoretical justification is provided in Section 3.1. ② **Partial-layer compression for SVD**: LLMs consist of a sequence of consecutive layers, where the output of each layer serves as the input to the next. As a result, any error introduced in earlier layers can propagate and accumulate through subsequent layers, leading to severe degradation in performance. To mitigate this, we propose compressing only the last few layers under a fixed overall compression ratio while keeping the earlier layers intact. This strategy ensures that the earlier layers remain error-free, thereby reducing the impact of error propagation.

Our key contributions can be summarized as follows:

- We introduce **residual compensation for SVD truncation**, a theoretically grounded compensation strategy. By leveraging the residual matrix generated during the SVD truncation, our strategy significantly reduces the overall truncation loss.
- We propose **partial-layer compression for SVD**, which compresses only the last few layers of the model under a fixed overall compression ratio. This strategy effectively reduces layer-wise error and mitigates error propagation.
- Extensive experiments on multiple LLMs (LLaMA, OPT, Mistral, and Vicuna) and benchmark datasets (both language modeling and zero-shot reasoning) demonstrate that ResSVD outperforms existing methods across a wide range of compression ratios.

2 Related Work

2.1 Techniques for Large Language Model Compression

The growing size of large language models (LLMs) has raised increasing concerns over their computational and memory demands. To address these challenges, a variety of model compression techniques have been proposed. Conventional approaches often require computationally expensive retraining, which is generally impractical due to the substantial computational cost associated with the massive size of LLMs. Consequently, recent efforts have shifted toward more resource-friendly post-training compression techniques [9, 10, 47]. Typically employed approaches include network pruning and weight quantization. And pruning techniques can be classified into unstructured and structured methods. Unstructured pruning removes individual weights based on importance scores. For example, SparseGPT [9] performs one-shot pruning using second-order approximations without retraining. However, since unstructured pruning retains the original matrix shape, it offers limited inference acceleration and requires specialized hardware. In contrast, structured pruning eliminates entire blocks or channels, enabling compatibility with conventional hardware platforms.

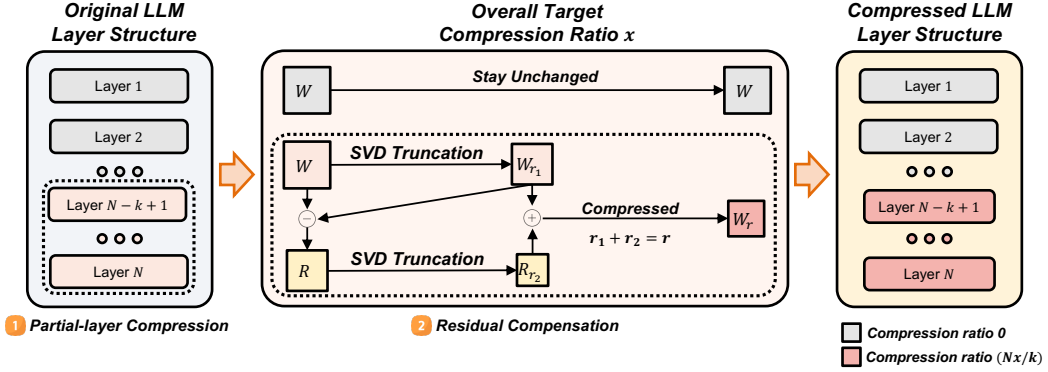


Figure 1: Framework of **ResSVD**. The last k layers are selected through **partial-layer compression** and compressed using **residual compensation** with calibration data. The first $(N - k)$ layers remain intact, while the last k layers are replaced by low-rank approximations.

LLM-Pruner [25] groups dependent linear projections into coupled structures, assigns each group a loss-aware importance score, prunes the least important groups, and applies LoRA fine-tuning to restore performance. Additionally, ZipLM [19] prioritizes pruning components that yield the worst trade-off between latency and loss, but this often causes notable performance degradation. Quantization provides another mainstream solution. GPTQ [10] gradually quantizes and updates each weight using the Hessian matrix to minimize the quantization error. AWQ [23] preserves important weight channels by selecting reparameterization coefficients via grid search. Furthermore, BiLLM [15] and ARB-LLM [22] push quantization to the 1-bit level, while still delivering impressive accuracy across downstream tasks. However, these techniques still cause significant performance degradation, especially at low bit-widths, due to the lack of weight and activation adaptation.

2.2 SVD-based Techniques for Compressing LLMs

Singular value decomposition (SVD) is a commonly employed technique for reducing matrix dimensionality by representing the original matrix as the product of two low-rank factor matrices. Recent research has demonstrated the potential of SVD-based LLM compression methods, but comprehensive exploration remains limited. The conventional SVD only aims to compress the original weight matrix, without accounting for the relative importance of individual parameters, leading to significant approximation errors. To address this issue, Hsu et al. [14] propose FWSVD, incorporating Fisher information to weight the importance of parameters. However, it relies on computationally intensive training and was originally applied only to small language models (e.g., BERT [8], ALBERT [20]). LoRD [18] first applies SVD to LLMs by grouping layers to improve efficiency. However, similar to conventional SVD, LoRD shares the limitation of overlooking input activations. To address this problem, Yuan et al. [42] introduce ASVD, which mitigates the impact of activation outliers by reshaping the weight matrix based on activation distribution, thereby enhancing the precision of the low-rank decomposition. Additionally, SVD-LLM [39] establishes a direct mapping between singular values and truncation loss, which means that truncating the smallest singular values leads to minimal truncation loss using a truncation-aware data whitening technique. More recently, AdaSVD [21] proposes an adaptive compensation method, iteratively updating matrices during truncation. Despite these advances, all existing methods ignore the residual matrix produced during SVD truncation, which can significantly compensate for the SVD truncation loss. Moreover, compressing only the last few layers of the model under a fixed target compression ratio can provide better performance for compressed models. However, existing methods compress all layers, either apply a uniform compression ratio across all layers or assign variable ratios based on layer-wise importance, which often results in sub-optimal performance.

3 ResSVD

The framework of **ResSVD** is illustrated in Figure 1. We first perform SVD to compress the last few layers of the model, while ensuring that the overall compression ratio is satisfied, and compute the

Algorithm 1 Pseudocode of **ResSVD**

Input: Original LLM: M , weight matrix: $\mathbf{W} \in \mathbb{R}^{m \times n}$, number of model layers: N , intermediate rank r_1 , step: s
Output: Compressed LLM M' by ResSVD

- 1: $CD \leftarrow$ Randomly collect calibration samples from the dataset
- 2: $\text{Set}_{\mathbf{W}} \leftarrow M$, $\text{Set}_{\mathbf{W}'} \leftarrow \emptyset$ \triangleright Initialize the sets of weight matrices
- 3: $k, R_l \leftarrow \text{PARTIAL-LAYER COMPRESSION}(M, N, R_o, s)$
- 4: **for** Layer i in original LLM M **do**
- 5: **if** $i \in [1, N - k]$ **then**
- 6: $\text{Set}_{\mathbf{W}'}(i) \leftarrow \text{Set}_{\mathbf{W}}(i)$ \triangleright Current weight matrices stay the same
- 7: **else**
- 8: $\mathbf{W}_i \leftarrow \text{Set}_{\mathbf{W}}(i)$, $\mathbf{S}_i \leftarrow \text{WHITENING}(\mathbf{W}_i, CD)$ \triangleright Initialize weight matrices to compress
- 9: $\text{Set}_{\mathbf{W}'}(i) \leftarrow \text{RESIDUAL COMPENSATION}(\mathbf{S}_i, k, R_l, r_1)$
- 10: **end if**
- 11: $\text{Set}_{\mathbf{W}'} \leftarrow \text{Set}_{\mathbf{W}'}(i) \cup \text{Set}_{\mathbf{W}'}$ \triangleright Append weight matrices after operation
- 12: **end for**
- 13: $M' \leftarrow \text{UPDATE}(M, CD, \text{Set}_{\mathbf{W}'})$
- 14: **return** M'

corresponding residual matrix. A second SVD is then applied to the residual matrix to obtain its low-rank approximation. The two truncated matrices are subsequently combined to construct the final compressed weight matrices. In Section 3.1, we first provide a theoretical analysis demonstrating how **residual compensation** effectively reduces truncation loss. Subsequently, in Section 3.2, we explain the benefits of **partial-layer compression** in mitigating error propagation. The pseudocode of ResSVD is shown in Algorithm 1, and the pseudocodes for residual compensation and partial-layer compression are provided in Appendix.

3.1 Residual Compensation for SVD Truncation

Preliminaries for SVD. Typical SVD-based LLM compression methods apply SVD to the original weight matrix $\mathbf{W} \in \mathbb{R}^{m \times n}$, and discard the smallest singular values to obtain a compressed low-rank approximation \mathbf{W}_r :

$$\mathbf{W} = \mathbf{U}\Sigma\mathbf{V}^T \approx \mathbf{U}_r\Sigma_r\mathbf{V}_r^T = \mathbf{W}_r, r < \min(m, n), \quad (1)$$

where $\mathbf{U}_r \in \mathbb{R}^{m \times r}$ and $\mathbf{V}_r^T \in \mathbb{R}^{r \times n}$ are composed of the top- r left and right singular vectors, respectively, and $\Sigma_r \in \mathbb{R}^{r \times r}$ is a diagonal matrix containing the corresponding singular values. Following prior post-training SVD-based works [39, 42], the optimization objective for SVD truncation in LLMs can be formulated as:

$$\hat{\mathbf{W}}_r = \arg \min_{\mathbf{W}_r} \|\mathbf{W}\mathbf{X} - \mathbf{W}_r\mathbf{X}\|_F, \quad (2)$$

$$\mathcal{L} = \|\mathbf{W}\mathbf{X} - \mathbf{W}_r\mathbf{X}\|_F = \|(\mathbf{W} - \mathbf{W}_r)\mathbf{X}\|_F, \quad (3)$$

where \mathbf{X} denotes the activation of \mathbf{W} given an input, and \mathcal{L} is the truncation loss measured by the Frobenius norm. Although previous works [14, 39, 42] have made significant progress in minimizing \mathcal{L} , they consistently overlook the residual matrix generated during truncation, despite its potential to compensate for the loss introduced by low-rank approximation.

Based on Equation 3, minimizing the truncation loss reduces to minimizing the discrepancy between the original weight matrix \mathbf{W} and its low-rank approximation \mathbf{W}_r . Accordingly, we reformulate the optimization objective as:

$$\hat{\mathbf{W}}_r = \arg \min_{\mathbf{W}_r} \|\mathbf{W} - \mathbf{W}_r\|. \quad (4)$$

Method Explanation for ResSVD. Given the original weight matrix \mathbf{W} and the target rank r , we decompose r into two components: an intermediate rank r_1 and a residual rank $r_2 = r - r_1$. The compression process consists of two SVD truncation steps. First, we apply SVD to \mathbf{W} and retain top- r_1 singular values to obtain a low-rank approximation: $\mathbf{W}_{r_1} = \mathbf{U}_{r_1}\Sigma_{r_1}\mathbf{V}_{r_1}^T$. The residual matrix is then computed as the difference between the original matrix and its rank- r_1

approximation: $\mathbf{R} = \mathbf{W} - \mathbf{W}_{r_1}$. We perform a second SVD on \mathbf{R} and retain the top- r_2 singular values: $\mathbf{R}_{r_2} = \mathbf{U}_{r_2} \mathbf{\Sigma}_{r_2} \mathbf{V}_{r_2}^T$. Finally, we obtain the compressed weight matrix by combining the two approximations: $\hat{\mathbf{W}}_r = \mathbf{W}_{r_1} + \mathbf{R}_{r_2} = \mathbf{U}_r \mathbf{\Sigma}_r \mathbf{V}_r^T$.

In this way, the residual-compensated compressed matrix $\hat{\mathbf{W}}_r$ provides a closer approximation to the original weight matrix \mathbf{W} than the directly truncated matrix \mathbf{W}_r , as proven in the theoretical analysis that follows.

Lemma 3.1. *Eckart-Young-Mirsky Theorem [13]. Given a matrix $\mathbf{A} \in \mathbb{R}^{m \times n}$ with singular values $\sigma_1(\mathbf{A}) \geq \sigma_2(\mathbf{A}) \geq \sigma_3(\mathbf{A}) \geq \dots \geq \sigma_{\min(m,n)}(\mathbf{A})$. The best rank- r approximation \mathbf{A}_r is given by:*

$$\mathbf{A}_r = \sum_{i=1}^r \sigma_i(\mathbf{A}) u_i(\mathbf{A}) v_i^T(\mathbf{A}), \quad (5)$$

and the truncation loss satisfies:

$$\|\mathbf{A} - \mathbf{A}_r\|_F^2 = \sum_{i=r+1}^{\min(m,n)} \sigma_i^2(\mathbf{A}). \quad (6)$$

As defined above, $\hat{\mathbf{W}}_r = \mathbf{W}_{r_1} + \mathbf{R}_{r_2}$. Let \mathcal{L}_C denote the truncation loss between the original matrix \mathbf{W} and the residual-compensated compressed matrix $\hat{\mathbf{W}}_r$. Then, by applying Lemma 3.1, we have:

$$\begin{aligned} \mathcal{L}_C &= \|\mathbf{W} - \hat{\mathbf{W}}_r\|_F^2 = \|\mathbf{W} - (\mathbf{W}_{r_1} + \mathbf{R}_{r_2})\|_F^2 = \|\mathbf{R} - \mathbf{R}_{r_2}\|_F^2 = \sum_{i=r_2+1}^{\text{rank}(\mathbf{R})} \sigma_i^2(\mathbf{R}), \\ &\text{rank}(\mathbf{R}) \leq \min(m, n) - r_1. \end{aligned} \quad (7)$$

Lemma 3.2. *If \mathbf{A}_r is the best rank- r approximation of $\mathbf{A} \in \mathbb{R}^{m \times n}$, and the residual is $\mathbf{B} = \mathbf{A} - \mathbf{A}_r$. Then we have:*

$$\sigma_i(\mathbf{B}) \leq \sigma_{r+i}(\mathbf{A}), 1 \leq i \leq \min(m, n) - r. \quad (8)$$

Theorem 3.3. *If \mathbf{W}_r is the rank- r direct truncation matrix from the original matrix \mathbf{W} , $\hat{\mathbf{W}}_r$ is the residual-compensated compressed matrix, then $\hat{\mathbf{W}}_r$ is closer to \mathbf{W} .*

Proof. The direct truncation loss \mathcal{L}_D between \mathbf{W} and \mathbf{W}_r is given by:

$$\mathcal{L}_D = \|\mathbf{W} - \mathbf{W}_r\|_F^2 = \sum_{i=r+1}^{\min(m,n)} \sigma_i^2(\mathbf{W}). \quad (9)$$

According to Lemma 3.2, the compensated truncation loss \mathcal{L}_C , as defined in Equation (7), is upper-bounded by:

$$\sum_{i=r_2+1}^{\text{rank}(\mathbf{R})} \sigma_i^2(\mathbf{R}) \leq \sum_{i=r_1+r_2+1}^{\min(m,n)} \sigma_i^2(\mathbf{W}) = \sum_{i=r+1}^{\min(m,n)} \sigma_i^2(\mathbf{W}). \quad (10)$$

Therefore, we obtain:

$$\boxed{\mathcal{L}_C \leq \mathcal{L}_D} \quad (11)$$

This proves that the compensated truncation loss \mathcal{L}_C is smaller than the direct truncation loss \mathcal{L}_D , which means that $\hat{\mathbf{W}}_r$ is closer to the original weight matrix \mathbf{W} . \square

3.2 Partial-layer Compression for SVD

Previous works [14, 21, 39, 42] compress all model layers even if they assign layer-specific ratios based on their relative importance, which often leads to a high layer-wise error, resulting in noticeable degradation in the performance of compressed models. We compare the layer-wise error of LLMs across four families with different layer selection strategies, the results are shown in Figure 3. There

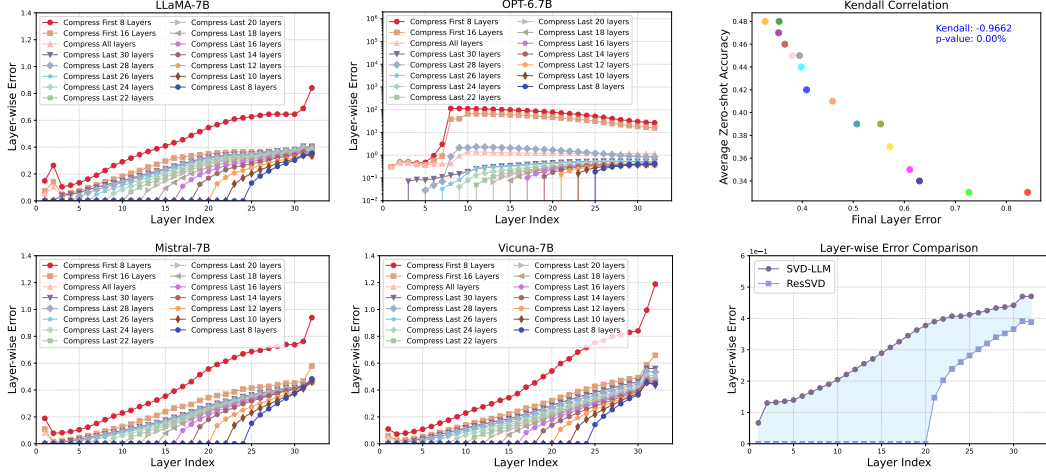


Figure 3: Layer-wise error comparison between original model and multiple LLM structures compressed by **ResSVD** with different layer selection strategies on WikiText-2 [27]. The overall compression ratio is 20%, and different layer selection strategies strictly adhere to the overall compression ratio constraint.

Figure 4: (Top) Kendall correlation. (Bottom) Layer-wise error comparison between ResSVD and SVD-LLM [39] under 20% compression ratio.

is a significant error propagation across multiple LLM families, where the error progressively accumulates layer by layer during the forward pass. This phenomenon is particularly pronounced when compressing the first 8 layers. To satisfy the overall compression ratio, a higher layer compression ratio (80% in this case) must be applied to these layers. Compressing the model at such an early stage introduces substantial approximation errors, which are then propagated through the remaining layers. Although the later layers are left uncompressed, the forward pass carries the accumulated error through the network. Consequently, in all evaluated LLM families, these early compressed layers exhibit the highest layer-wise error across model layers. In contrast, when only compressing the last few layers, the earlier layers remain untouched with zero error. Although the compression ratio for selected layers is relatively high, leading to slightly faster error accumulation, the overall error remains significantly lower than that of compressing all layers.

Interestingly, we observe that although the final-layer error converges to a narrow range regardless of how many of the last layers are compressed, the differences within this range still exhibit a strong influence on model performance. As illustrated in the top figure of Figure 4, there is a strong correlation between the final-layer error and the average zero-shot accuracy. Motivated by this observation, we select the number of last layers to compress by minimizing the final-layer error, and the layer compression ratio R_o satisfies:

$$R_l = (N \cdot R_o)/k, k \in \{1, 2, \dots, N-1 \mid R_l < 1\}, \quad (12)$$

where N is the number of model layers, R_l represents the overall compression ratio. As shown in the bottom figure of Figure 4, compared to SVD-LLM [39], our strategy significantly reduces layer-wise error across all model layers and mitigates error propagation.

4 Experiments

4.1 Setups

Baselines. We compare with four baselines in post-training setting, i.e., without re-training of the model parameters: conventional SVD, ASVD [42], SVD-LLM [39], and AdaSVD [21].

Models and Datasets. We evaluate **ResSVD** on ten models spanning four LLM families: LLaMA-7B [36], LLaMA-13B [36], LLaMA-30B [36], LLaMA-2-7B [37], LLaMA-2-13B [37], OPT-6.7B [44], OPT-13B [44], OPT-30B [44], Mistral-7B [16], Vicuna-7B [5]. For language modeling, we use three benchmark datasets: WikiText-2 [27], PTB [26], and C4 [30]. For zero-shot reasoning

Table 1: Overall performance of LLaMA-7B [36] compressed by **ResSVD** and baselines under 20% to 60% compression ratios ("RATIO"), including performance on three language modeling datasets (measured by perplexity (\downarrow)) and zero-shot performance on seven common sense reasoning datasets (measured by individual and average accuracy (\uparrow)). The best results are marked in **bold**. Blue arrows within parentheses highlight the relative improvement over the second-best method.

RATIO	METHOD	WikiText-2 \downarrow	PTB \downarrow	C4 \downarrow	Openb. \uparrow	ARC_e \uparrow	WinoG. \uparrow	HellaS. \uparrow	ARC_c \uparrow	PIQA \uparrow	MathQA \uparrow	Average \uparrow
-	Original	5.67	8.80	7.63	0.28	0.67	0.67	0.56	0.38	0.78	0.27	0.52
20%	SVD	20082.86	20338.96	18784.20	0.14	0.27	0.51	0.26	0.21	0.53	0.21	0.30
	ASVD [42]	9.27	<u>15.09</u>	<u>13.68</u>	<u>0.25</u>	0.53	0.60	0.41	0.27	0.68	<u>0.25</u>	<u>0.43</u>
	SVD-LLM [39]	7.89	16.54	15.92	0.23	<u>0.56</u>	<u>0.62</u>	<u>0.42</u>	<u>0.29</u>	<u>0.69</u>	0.23	<u>0.43</u>
30%	ResSVD	7.47 (\downarrow 5%)	12.27 (\downarrow 19%)	12.22 (\downarrow 11%)	0.25	0.59	0.67	0.47	0.34	0.71	0.25	0.47 (\uparrow 9%)
	SVD	13155.97	17354.46	21012.91	0.13	0.26	0.51	0.25	0.21	0.54	0.21	0.30
	ASVD [42]	222.98	586.79	148.79	0.15	0.32	0.53	0.30	0.21	0.59	0.21	0.33
40%	SVD-LLM [39]	9.52	28.97	26.38	0.20	0.49	0.59	0.37	0.27	0.65	0.22	0.40
	ResSVD	9.52 (\downarrow)	20.31 (\downarrow 30%)	18.29 (\downarrow 31%)	0.23	0.54	0.63	0.41	0.30	0.67	0.23	0.43 (\uparrow 8%)
	SVD	52326.99	59859.41	47643.04	0.15	0.25	0.51	0.25	0.21	0.52	0.20	0.30
50%	ASVD [42]	5262.11	8806.33	6522.61	0.14	0.26	0.49	0.26	<u>0.22</u>	0.53	0.20	0.30
	SVD-LLM [39]	13.83	57.07	48.47	0.19	0.41	0.58	<u>0.32</u>	<u>0.22</u>	0.59	<u>0.22</u>	<u>0.36</u>
	ResSVD	12.92 (\downarrow 7%)	46.93 (\downarrow 18%)	30.51 (\downarrow 37%)	0.19	0.44	0.60	0.35	0.27	0.62	0.24	0.39 (\uparrow 8%)
60%	SVD	130388.72	86721.38	79853.46	0.16	0.26	0.49	0.25	0.22	0.52	0.18	0.30
	ASVD [42]	62726.86	117959.06	77773.84	0.13	0.25	0.48	0.25	<u>0.22</u>	0.53	0.21	0.30
	SVD-LLM [39]	24.05	<u>150.58</u>	141.87	0.16	<u>0.34</u>	<u>0.55</u>	<u>0.29</u>	0.21	<u>0.56</u>	<u>0.22</u>	<u>0.33</u>
	ResSVD	22.41 (\downarrow 7%)	128.80 (\downarrow 14%)	83.80 (\downarrow 41%)	0.16	0.36	0.58	0.32	0.23	0.59	0.22	0.35 (\uparrow 6%)
	SVD	52326.99	59859.41	47643.04	0.15	0.25	0.51	0.25	<u>0.21</u>	0.52	0.20	0.30
	ASVD [42]	16221.43	20119.36	16561.39	0.13	0.26	0.50	0.25	0.23	0.53	0.18	0.30
	SVD-LLM [39]	53.20	378.19	310.17	0.12	0.29	0.52	0.28	0.20	<u>0.55</u>	0.22	0.31
	ResSVD	48.67 (\downarrow 9%)	323.74 (\downarrow 14%)	260.06 (\downarrow 16%)	<u>0.14</u>	0.30	0.53	0.28	<u>0.21</u>	0.55	<u>0.21</u>	0.32 (\uparrow 3%)

and understanding, we evaluate on seven tasks within the *LM-Evaluation-Harness* framework²: OpenbookQA [28], WinoGrande [32], HellaSwag [43], PIQA [3], MathQA [1], ARC_e and ARC_c [7].

Implementation Details. To facilitate a fair comparison, we follow the protocols of ASVD, SVD-LLM, and AdaSVD, randomly selecting 256 calibration samples with a sequence length of 2048 from WikiText-2. We then apply data whitening prior to performing SVD truncation. All results are reproduced by re-running their respective open-source codebases, except for AdaSVD, whose results are directly taken from the original paper due to the lack of released code. All methods are all implemented with PyTorch³ and Transformers⁴ on NVIDIA A100 GPUs.

4.2 Results

We evaluate the overall performance of ResSVD from three aspects: ① **Effectiveness under different compression ratios** (ranging from 20% to 60% in increments of 10%), ② **Scalability when applied to larger-scale models**, and ③ **Generalizability across diverse LLM families**. In addition, qualitative results, such as generated contents produced by compressed models, are provided in Appendix, offering a more intuitive and direct comparison.

Performance under different compression ratios. We evaluate the performance of LLaMA-7B [36] and LLaMA-2-7B [37] compressed by ResSVD, conventional SVD, and existing post-training baselines under compression ratios ranging from 20% to 60% across 10 benchmark datasets. The results for LLaMA-7B are presented in Table 1, while those for LLaMA-2-7B are provided in Appendix. On the three language modeling datasets, WikiText-2 [27], PTB [26], and C4 [30], ResSVD consistently outperforms all baselines across evaluated compression ratios. In particular, on PTB and C4, the improvements are more pronounced, suggesting that ResSVD exhibits stronger generalization capability. More importantly, under a relatively high compression ratio (e.g., 50%), ResSVD still achieves substantial perplexity reductions compared to the existing best-performing baseline SVD-LLM [39]: 7% on WikiText-2, 14% on PTB, and 41% on C4. This demonstrates that ResSVD maintains an obvious performance advantage even under aggressive compression. In addition, on seven common sense reasoning datasets, ResSVD surpasses the existing best baseline on the majority of datasets, with an average accuracy gain of up to 9%, and a minimum improvement of 3% improvement, further highlighting its robustness and overall effectiveness.

²<https://github.com/EleutherAI/lm-evaluation-harness>

³<https://github.com/pytorch/pytorchandHuggingFace>

⁴<https://github.com/huggingface/transformers>

Performance on Different LLM families. To evaluate the generalization ability of ResSVD, we apply it to four LLMs from different families, including OPT-6.7B [44], LLaMA-2-7B, Mistral-7B [16], and Vicuna-7B [5]. As shown in Table 3, under 30% compression ratio, ResSVD consistently outperforms all baselines across three language modeling benchmarks across these diverse architectures. The most significant relative improvement reaches 75% on LLaMA-2-7B. Moreover, the best overall improvement is achieved on Mistral-7B, with perplexity reductions of 71% on WikiText-2, 45% on PTB, and 46% on C4. We reproduce ASVD [42] and SVD-LLM [39] using their public codebases. While ASVD fails in certain cases due to numerical instability (denoted as NaN in the table), ResSVD consistently maintains stable and reliable performance.

Table 2: Perplexity (\downarrow) of larger-scale LLMs under 20% compression ratio on PTB [26].

METHOD	LLaMA-13B	LLaMA-30B	LLaMA-2-13B	OPT-13B	OPT-30B
SVD	1878.04	555.55	5464.57	1552.55	250.49
ASVD [42]	12.42	31.36	81.00	36.47	30.95
SVD-LLM [39]	12.17	9.10	88.13	14.86	12.94
ResSVD	9.70	8.41	66.47	13.22	12.89

Table 3: Perplexity (\downarrow) of different LLM structures under 30% compression ratio.

MODEL	METHOD	WikiText-2 \downarrow	PTB \downarrow	C4 \downarrow
OPT-6.7B	SVD	116067.28	86760.50	168165.89
	ASVD [42]	26.67	71.36	44.51
	SVD-LLM [39]	28.03	37.46	40.35
LLaMA-2-7B	ResSVD	17.10 (\downarrow 36%)	27.24 (\downarrow 27%)	38.40 (\downarrow 15%)
	SVD	30373.39	48930.94	36905.54
	ASVD [42]	984.03	NaN	NaN
Mistral-7B	SVD	10.66	292.90	34.96
	ASVD [42]	48.94	193.22	56.55
	ResSVD	10.32 (\downarrow 3%)	73.04 (\downarrow 75%)	23.28 (\downarrow 13%)
Vicuna-7B	SVD	59569.54	57830.63	78168.24
	ASVD [42]	221.66	927.15	266.04
	SVD-LLM [39]	140.99	193.22	56.55
ResSVD	ResSVD	14.09 (\downarrow 71%)	105.37 (\downarrow 45%)	30.72 (\downarrow 46%)
	SVD	24835.33	24510.90	29368.55
	ASVD [42]	106.32	NaN	NaN
SVD-LLM [39]	SVD-LLM [39]	12.42	104.27	39.55
	ResSVD	11.57 (\downarrow 7%)	69.28 (\downarrow 34%)	27.24 (\downarrow 31%)

Performance on Larger Scale LLMs. To examine the scalability and robustness of ResSVD, we evaluate its performance on larger scale LLMs from two representative LLM families: LLaMA (including LLaMA-13B, LLaMA-30B, and LLaMA-2-13B) and OPT (OPT-13B and OPT-30B). As presented in Table 2, ResSVD consistently achieves superior performance over existing baselines under 20% compression ratio, demonstrating robust effectiveness across varying model scales.

4.3 Ablation Study

In this section, we present extensive ablation study results to assess the effectiveness and robustness of **ResSVD** from three key perspectives. ① **Effectiveness of residual compensation and partial-layer compression:** We evaluate the individual contributions of the residual compensation mechanism and partial-layer compression. ③ **Impact of layer selection strategy:** We show that restricting compression to the last few layers mitigates error accumulation and consistently improves performance. ③ **Impact of calibration data:** We analyze the effects of both calibration sample size and dataset choice on the performance of compressed models.

Effectiveness of residual compensation and partial-layer compression. As shown in Table 4, we conduct ablation studies to evaluate the individual contributions of residual compensation (REC) and partial-layer compression (PLC). Specifically, the left table presents the results for REC under multiple compression ratios. Incorporating REC consistently reduces perplexity across all settings, and ResSVD achieves the best performance across all datasets and baselines. The right table reports the results for PLC. Without PLC, perplexity on WikiText-2 [27] increases slightly, indicating the effect of cumulative error. In contrast, applying PLC consistently enhances performance, further amplifying the benefits of REC. These results confirm that PLC is essential for mitigating error propagation. More ablation results are provided in Appendix.

Impact of layer selection strategy. We compare the performance of LLaMA-7B [36] under 20% compression ratio with different layer selection strategies. The results are shown in Table 5. We observe that the performance of the compressed model varies significantly depending on which layers are selected for compression. The worst performance is observed when compressing the first 8 layers, primarily because the compression ratio per layer becomes excessively high, and error accumulation begins from the first layer. Across all configurations, compressing the last 16 layers yields the best overall performance. However, as more layers are compressed, the performance gradually declines, which can be attributed to increased cumulative approximation error.

Impact of calibration data. The selection of calibration data plays a critical role in post-training compression. To assess this, we vary both the number of calibration samples and the choice of

Table 4: Ablation results of residual compensation (REC) and partial-layer compression (PLC) on LLaMA-7B [36] under compression ratios 20% and 30%. More ablation results are in Appendix.

(a) REC			(b) PLC		
COMP. RATIO	METHOD	REC	WikiText-2 \downarrow	PTB \downarrow	C4 \downarrow
20%	SVD	X	20082.86	20338.96	18784.20
	ASVD [42]	X	9.27	15.09	13.68
	SVD-LLM [39]	X	7.89	16.54	15.92
	ResSVD	X	7.93	13.68	13.72
30%	SVD	X	13155.97	17354.46	21012.91
	ASVD [42]	X	222.98	586.79	148.79
	SVD-LLM [39]	X	9.52	28.97	26.38
	ResSVD	X	9.60	26.12	20.97
	ResSVD	✓	9.52	20.31	18.29

Table 5: Performance of compressed LLaMA-7B [36] with various layer selection strategies.

COMP. LAYERS	LAYER COMP. RATIO	WikiText-2 \downarrow	PTB \downarrow	C4 \downarrow	Average \uparrow
First 8	80%	16.56	37.58	46.16	0.33
Last 8	80%	10.69	19.26	16.06	0.38
Last 12	53%	8.49	14.04	13.50	0.44
Last 16	40%	7.47	12.27	12.22	0.47
Last 20	32%	8.07	14.19	13.68	0.46
Last 24	27%	8.08	14.66	13.94	0.45
Last 28	23%	8.21	16.04	14.98	0.45
Last 32	20%	8.27	16.00	15.78	0.44

Table 6: Perplexity (\downarrow) and zero-shot average accuracy (\uparrow) of LLaMA-7B [36] compressed by **ResSVD** under 20% compression ratio while using different calibration datasets.

CALIBRATION DATASET	WikiText-2 \downarrow	PTB \downarrow	C4 \downarrow	Avg \uparrow
WikiText-2 [27]	7.47	12.27	12.22	0.47
PTB [26]	9.86	9.54	12.70	0.45
C4 [30]	10.05	12.42	10.94	0.47

calibration datasets. Figure 6 shows the perplexity on WikiText-2 [27] and average zero-shot accuracy under 20% compression ratio. While performance slightly improves with more calibration samples, the gains are modest, indicating that ResSVD remains robust even with limited calibration data. Moreover, Table 6 shows that the best results are achieved when the calibration and evaluation datasets align, suggesting that domain consistency enhances compression quality.

4.4 Efficiency Results

ResSVD not only preserves competitive model performance but also delivers significant inference speedup on hardware. We evaluate the throughput of compressed models on an NVIDIA A100 GPU, with results shown in Figure 7. Models compressed by ResSVD consistently achieve faster inference than those compressed by SVD-LLM [39]. Moreover, the speedup becomes increasingly significant as the batch size grows, indicating that ResSVD scales more efficiently under larger workloads. These findings highlight the practical efficiency of ResSVD in enabling faster inference while maintaining accuracy, making it well-suited for deployment in resource-constrained environments.

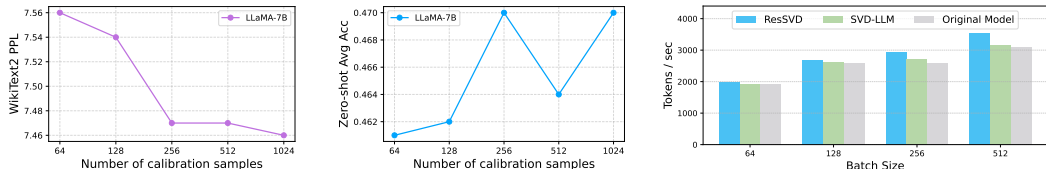


Figure 6: Impact of the number of calibration data samples on LLaMA-7B [36] under 20% compression ratio. (Left) Perplexity (\downarrow). (Right) Average accuracy (\uparrow).

Figure 7: Throughput of LLaMA-7B [36] and its 40% compressed versions. The sequence length is 32.

5 Conclusion

In this work, we propose **ResSVD**, a novel post-training SVD-based compression method for large language models. ResSVD effectively leverages the residual matrix resulting from SVD truncation

to reduce the truncation loss and enhance layer-wise reconstruction accuracy. Furthermore, it selectively compresses only the last few layers of the model under a fixed overall compression ratio, thereby significantly mitigating error propagation across the model. Extensive experiments across various LLM families and benchmark datasets demonstrate that ResSVD consistently outperforms existing SVD-based baselines across various settings. These results highlight the effectiveness and generalizability of ResSVD in enabling efficient LLM deployment.

References

- [1] A. Amini, S. Gabriel, S. Lin, R. Koncel-Kedziorski, Y. Choi, and H. Hajishirzi. Mathqa: Towards interpretable math word problem solving with operation-based formalisms. In *NAACL-HLT*, 2019.
- [2] J. Bai, S. Bai, Y. Chu, Z. Cui, K. Dang, X. Deng, Y. Fan, W. Ge, Y. Han, F. Huang, et al. Qwen technical report. *arXiv preprint arXiv:2309.16609*, 2023.
- [3] Y. Bisk, R. Zellers, R. L. Bras, J. Gao, and Y. Choi. PIQA: reasoning about physical common-sense in natural language. In *AAAI*, 2020.
- [4] T. B. Brown, B. Mann, N. Ryder, M. Subbiah, J. Kaplan, P. Dhariwal, A. Neelakantan, P. Shyam, G. Sastry, A. Askell, S. Agarwal, A. Herbert-Voss, G. Krueger, T. Henighan, R. Child, A. Ramesh, D. M. Ziegler, J. Wu, C. Winter, C. Hesse, M. Chen, E. Sigler, M. Litwin, S. Gray, B. Chess, J. Clark, C. Berner, S. McCandlish, A. Radford, I. Sutskever, and D. Amodei. Language models are few-shot learners. In *NeurIPS*, 2020.
- [5] W.-L. Chiang, Z. Li, Z. Lin, Y. Sheng, Z. Wu, H. Zhang, L. Zheng, S. Zhuang, Y. Zhuang, J. E. Gonzalez, et al. Vicuna: An open-source chatbot impressing gpt-4 with 90%* chatgpt quality. See <https://vicuna.lmsys.org>, 2(3):6, 2023.
- [6] A. Chowdhery, S. Narang, J. Devlin, M. Bosma, G. Mishra, A. Roberts, P. Barham, H. W. Chung, C. Sutton, S. Gehrmann, P. Schuh, K. Shi, S. Tsvyashchenko, J. Maynez, A. Rao, P. Barnes, Y. Tay, N. Shazeer, V. Prabhakaran, E. Reif, N. Du, B. Hutchinson, R. Pope, J. Bradbury, J. Austin, M. Isard, G. Gur-Ari, P. Yin, T. Duke, A. Levskaya, S. Ghemawat, S. Dev, H. Michalewski, X. Garcia, V. Misra, K. Robinson, L. Fedus, D. Zhou, D. Ippolito, D. Luan, H. Lim, B. Zoph, A. Spiridonov, R. Sepassi, D. Dohan, S. Agrawal, M. Omernick, A. M. Dai, T. S. Pillai, M. Pellat, A. Lewkowycz, E. Moreira, R. Child, O. Polozov, K. Lee, Z. Zhou, X. Wang, B. Saeta, M. Diaz, O. Firat, M. Catasta, J. Wei, K. Meier-Hellstern, D. Eck, J. Dean, S. Petrov, and N. Fiedel. Palm: Scaling language modeling with pathways. *Journal of Machine Learning Research*, 24(240):1–113, 2023.
- [7] P. Clark, I. Cowhey, O. Etzioni, T. Khot, A. Sabharwal, C. Schoenick, and O. Tafjord. Think you have solved question answering? try arc, the AI2 reasoning challenge. In *CVPR*, 2023.
- [8] J. Devlin, M. Chang, K. Lee, and K. Toutanova. BERT: pre-training of deep bidirectional transformers for language understanding. In *NAACL-HLT*, 2019.
- [9] E. Frantar and D. Alistarh. Sparsegpt: Massive language models can be accurately pruned in one-shot. In *ICML*, 2023.
- [10] E. Frantar, S. Ashkboos, T. Hoefer, and D. Alistarh. GPTQ: accurate post-training quantization for generative pre-trained transformers. *arXiv preprint arXiv:2210.17323*, 2022.
- [11] S. Gao, C.-H. Lin, T. Hua, Z. Tang, Y. Shen, H. Jin, and Y.-C. Hsu. Disp-llm: Dimension-independent structural pruning for large language models. In *NeurIPS*, 2024.
- [12] Y. Gu, L. Dong, F. Wei, and M. Huang. Minillm: Knowledge distillation of large language models. In *ICLR*, 2024.
- [13] R. A. Horn and C. R. Johnson. *Matrix analysis*. Cambridge university press, 2012.
- [14] Y. Hsu, T. Hua, S. Chang, Q. Lou, Y. Shen, and H. Jin. Language model compression with weighted low-rank factorization. In *ICLR*, 2022.
- [15] W. Huang, Y. Liu, H. Qin, Y. Li, S. Zhang, X. Liu, M. Magno, and X. Qi. Billm: Pushing the limit of post-training quantization for llms. In *ICML*, 2024.
- [16] A. Q. Jiang, A. Sablayrolles, A. Mensch, C. Bamford, D. S. Chaplot, D. de Las Casas, F. Bressand, G. Lengyel, G. Lample, L. Saulnier, L. R. Lavaud, M. Lachaux, P. Stock, T. L. Scao, T. Lavril, T. Wang, T. Lacroix, and W. E. Sayed. Mistral 7b. *arXiv preprint arXiv:2310.06825*, 2023.

[17] J. Kaplan, S. McCandlish, T. Henighan, T. B. Brown, B. Chess, R. Child, S. Gray, A. Radford, J. Wu, and D. Amodei. Scaling laws for neural language models. *arXiv preprint arXiv:2001.08361*, 2020.

[18] A. Kaushal, T. Vaidhya, and I. Rish. LORD: low rank decomposition of monolingual code llms for one-shot compression. *arXiv preprint arXiv:2309.14021*, 2023.

[19] E. Kurtic, E. Frantar, and D. Alistarh. Ziplm: Inference-aware structured pruning of language models. In *NeurIPS*, 2023.

[20] Z. Lan, M. Chen, S. Goodman, K. Gimpel, P. Sharma, and R. Soricut. ALBERT: A lite BERT for self-supervised learning of language representations. In *ICLR*, 2020.

[21] Z. Li, M. Xia, J. Zhang, Z. Hui, L. Kong, Y. Zhang, and X. Yang. Adasvd: Adaptive singular value decomposition for large language models. *arXiv preprint arXiv:2502.01403*, 2025.

[22] Z. Li, X. Yan, T. Zhang, H. Qin, D. Xie, J. Tian, L. Kong, Y. Zhang, X. Yang, et al. ARB-LLM: alternating refined binarizations for large language models. *arXiv preprint arXiv:2410.03129*, 2024.

[23] J. Lin, J. Tang, H. Tang, S. Yang, W. Chen, W. Wang, G. Xiao, X. Dang, C. Gan, and S. Han. AWQ: activation-aware weight quantization for on-device LLM compression and acceleration. In *MLSys*, 2024.

[24] A. Liu, B. Feng, B. Xue, B. Wang, B. Wu, C. Lu, C. Zhao, C. Deng, C. Zhang, C. Ruan, et al. Deepseek-v3 technical report. *arXiv preprint arXiv:2412.19437*, 2024.

[25] X. Ma, G. Fang, and X. Wang. Llm-pruner: On the structural pruning of large language models. In *NeurIPS*, 2023.

[26] M. P. Marcus, B. Santorini, and M. A. Marcinkiewicz. Building a large annotated corpus of english: The penn treebank. *Computational linguistics*, 19(2):313–330, 1993.

[27] S. Merity, C. Xiong, J. Bradbury, and R. Socher. Pointer sentinel mixture models. In *ICLR*, 2017.

[28] T. Mihaylov, P. Clark, T. Khot, and A. Sabharwal. Can a suit of armor conduct electricity? A new dataset for open book question answering. In *EMNLP*, 2018.

[29] D. A. Patterson, J. Gonzalez, U. Hözle, Q. V. Le, C. Liang, L. Munguia, D. Rothchild, D. R. So, M. Texier, and J. Dean. The carbon footprint of machine learning training will plateau, then shrink. *Computer*, 55(7):18–28, 2022.

[30] C. Raffel, N. Shazeer, A. Roberts, K. Lee, S. Narang, M. Matena, Y. Zhou, W. Li, and P. J. Liu. Exploring the limits of transfer learning with a unified text-to-text transformer. *Journal of machine learning research*, 21(140):1–67, 2020.

[31] R. Saha, N. Sagan, V. Srivastava, A. Goldsmith, and M. Pilanci. Compressing large language models using low rank and low precision decomposition. In *NeurIPS*, 2024.

[32] K. Sakaguchi, R. L. Bras, C. Bhagavatula, and Y. Choi. Winogrande: an adversarial winograd schema challenge at scale. *Communications of the ACM*, 64(9):99–106, 2021.

[33] Y. Sheng, L. Zheng, B. Yuan, Z. Li, M. Ryabinin, B. Chen, P. Liang, C. Ré, I. Stoica, and C. Zhang. Flexgen: High-throughput generative inference of large language models with a single GPU. In *ICML*, 2023.

[34] E. Strubell, A. Ganesh, and A. McCallum. Energy and policy considerations for modern deep learning research. In *AAAI*, 2020.

[35] M. Sun, Z. Liu, A. Bair, and J. Z. Kolter. A simple and effective pruning approach for large language models. In *ICLR*, 2024.

[36] H. Touvron, T. Lavril, G. Izacard, X. Martinet, M. Lachaux, T. Lacroix, B. Rozière, N. Goyal, E. Hambro, F. Azhar, A. Rodriguez, A. Joulin, E. Grave, and G. Lample. Llama: Open and efficient foundation language models. *arXiv preprint arXiv:2302.13971*, 2023.

[37] H. Touvron, L. Martin, K. Stone, P. Albert, A. Almahairi, Y. Babaei, N. Bashlykov, S. Batra, P. Bhargava, S. Bhosale, D. Bikel, L. Blecher, C. Canton-Ferrer, M. Chen, G. Cucurull, D. Esiobu, J. Fernandes, J. Fu, W. Fu, B. Fuller, C. Gao, V. Goswami, N. Goyal, A. Hartshorn, S. Hosseini, R. Hou, H. Inan, M. Kardas, V. Kerkez, M. Khabsa, I. Kloumann, A. Korenev, P. S. Koura, M. Lachaux, T. Lavril, J. Lee, D. Liskovich, Y. Lu, Y. Mao, X. Martinet, T. Mihaylov, P. Mishra, I. Molybog, Y. Nie, A. Poulton, J. Reizenstein, R. Rungta, K. Saladi, A. Schelten, R. Silva, E. M. Smith, R. Subramanian, X. E. Tan, B. Tang, R. Taylor, A. Williams, J. X. Kuan, P. Xu, Z. Yan, I. Zarov, Y. Zhang, A. Fan, M. Kambadur, S. Narang, A. Rodriguez, R. Stojnic, S. Edunov, and T. Scialom. Llama 2: Open foundation and fine-tuned chat models. *arXiv preprint arXiv:2307.09288*, 2023.

[38] W. Wang, W. Chen, Y. Luo, Y. Long, Z. Lin, L. Zhang, B. Lin, D. Cai, and X. He. Model compression and efficient inference for large language models: A survey. *arXiv preprint arXiv:2402.09748*, 2024.

[39] X. Wang, Y. Zheng, Z. Wan, and M. Zhang. SVD-LLM: truncation-aware singular value decomposition for large language model compression. In *ICLR*, 2025.

[40] X. Xu, M. Li, C. Tao, T. Shen, R. Cheng, J. Li, C. Xu, D. Tao, and T. Zhou. A survey on knowledge distillation of large language models. *arXiv preprint arXiv:2402.13116*, 2024.

[41] C. Yang, W. Lu, Y. Zhu, Y. Wang, Q. Chen, C. Gao, B. Yan, and Y. Chen. Survey on knowledge distillation for large language models: Methods, evaluation, and application. *ACM Transactions on Intelligent Systems and Technology*, 2024.

[42] Z. Yuan, Y. Shang, Y. Song, Q. Wu, Y. Yan, and G. Sun. ASVD: activation-aware singular value decomposition for compressing large language models. *arXiv preprint arXiv:2312.05821*, 2023.

[43] R. Zellers, A. Holtzman, Y. Bisk, A. Farhadi, and Y. Choi. Hellaswag: Can a machine really finish your sentence? In *ACL*, 2019.

[44] S. Zhang, S. Roller, N. Goyal, M. Artetxe, M. Chen, S. Chen, C. Dewan, M. T. Diab, X. Li, X. V. Lin, T. Mihaylov, M. Ott, S. Shleifer, K. Shuster, D. Simig, P. S. Koura, A. Sridhar, T. Wang, and L. Zettlemoyer. OPT: open pre-trained transformer language models. *arXiv preprint arXiv:2205.01068*, 2022.

[45] S. Zhang, X. Zhang, Z. Sun, Y. Chen, and J. Xu. Dual-space knowledge distillation for large language models. In *EMNLP*, 2024.

[46] Z. Zhou, X. Ning, K. Hong, T. Fu, J. Xu, S. Li, Y. Lou, L. Wang, Z. Yuan, X. Li, et al. A survey on efficient inference for large language models. *arXiv preprint arXiv:2404.14294*, 2024.

[47] X. Zhu, J. Li, Y. Liu, C. Ma, and W. Wang. A survey on model compression for large language models. In *ACL*, 2024.